Building Simulation 2009

Eleventh International IBPSA Conference
Glasgow, Scotland
July 27-30, 2009

MODELLING BUOYANCY INDUCED FLOWS OF PASSIVE COOLING SYSTEMS

Pedro Correia da Silva[1], Vítor Leal[1] and J. Correia da Silva[2]

[1] Mechanical Engineering Department
Faculdade de Engenharia da Universidade do Porto
Rua Dr. Roberto Frias, s.n., 4200-465 Porto – Portugal
pedro.correia.silva@fe.up.pt, vleal@fe.up.pt
[2] Universidade de Évora, Portugal

ABSTRACT

The main objective of this study is to develop and validate a systematic methodology to model a system of buried pipes, assisted by a solar chimney to promote the natural ventilation, in the whole building simulation software ESP-r (Clarke 2001), from a software user perspective. This development was supported by monitored data collected at an experimental site in Évora, Portugal.

A multi-zone ESP-r model was built to represent the entire installation using a nodal airflow network approach.

A sensitivity study was performed, trying to calibrate the simulation model to yield results compatible with the measurements. The localized loss coefficients in the airflow network were found to be the major influence for the model performance. The influence of convective heat transfer coefficients related to the airflow velocity was also considered and found to have a relevant impact too. Overall, it was found that without changes to the source code it was possible to capture most of the system behaviour, although some non-negligible differences between the simulation and the experiment remained.

INTRODUCTION

The interest for the integration of buried pipes in buildings has risen in recent years. Although *Computational Fluid Dynamics* (CFD) seems to be the most accurate tool for the system optimization, the assessment of the energy impact of the system over the year must be performed with whole building simulation tools. The issue of modelling in whole building simulation tools is thus of great importance.

This study has as main objective the assessment of the best approaches and calibration coefficients to model buried pipes ventilation systems coupled with solar chimneys and was performed in the perspective of a software user, i.e. no changes were made the source code.

For that purpose, the following steps are included in this study:

- The development of a simulation model to quantify the cooling effect of soil heat exchangers and passive cooling and to estimate the natural ventilation through a solar chimney;
- The improvement and validation of the developed simulation model using experimental data from a installation built in Évora - Portugal.

EXPERIMENTAL INSTALLATION

The experimental installation that supports the current study was built in the campus of the University of Évora. The intervention has included the construction of a room, adjacent to the existent building, with two chimneys – a normal chimney and a solar chimney (figure 1) and also a buried pipe with one extreme open to the exterior (figure 2), and the other connected to the test room.

The experimental installation is composed of two different zones. One of them is the room object of monitoring, the test room with an area of 10.5 m^2 and a volume of 34.2m^3, and the other, adjacent to the first, works as an entrance hall. Two chimneys were built in the test room: a conventional one (closed during the monitoring period) and a solar chimney. The solar chimney is south oriented and has a single glazing with the external surface of the interior wall coated by a black aluminum sheet.

Figure 1: Showing the solar chimney

Figure 2: Showing the outdoor entrance of the buried pipes

The pipe that integrates the cooling system has an internal diameter of 300mm and total horizontal length of 30m. The pipe was built in light concrete (wall thickness of 30mm) and was buried in a depth of 3m. The vertical connection from the horizontal concrete pipe to the test room was made with a PVC pipe. During the construction process, the pipe was covered by sand (about 200mm) and the remaining depth by common earth. In table 1 are presented the envelope characteristics of the test room.

The monitoring procedures of the experimental installation took place for two months (July and August of 2007). The monitoring included the indoor temperature and relative humidity of the test room, the temperature and relative humidity of the buried pipes air at the entrance of the test room, the temperature of the buried pipes outside surface and the air temperature measured along the length of the buried pipes. The outdoor climate conditions were also registered, such as the ambient temperature, the relative humidity, the solar radiation, the velocity and direction of the wind.

Table 1: Heat transfer properties of the test room envelope

Construction	**Construction elements**	**U ($W/m^2.°C$)**
Exterior wall	Brick (110mm), EPS (40mm), brick (110mm)	0.57
Interior wall	Brick (110mm)	1.10
Floor	Concrete (150mm), gravel (150mm)	4.17
Roof	Concrete (150mm), EPS (60mm), gravel (200mm)	0.41
Window (solar chimney)	Single glazing, solar factor = 0.85	5.75

SIMULATION MODEL

A simulation model of the experimental installation was developed in *Environmental Systems Performance - research* (ESP-r) that has the ability of combining, at the same model, the heat transfer building simulation and the airflow networks associated with each building element. The figure 3 has a graphical representation of the developed simulation model.

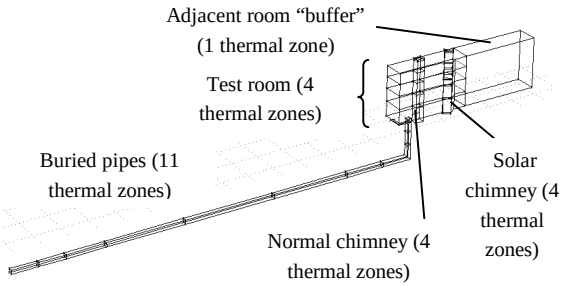

Figure 3: Simulation model of the experimental installation

A multi-zone air flow network model reproduced the entire installation, taking into account the thermal stratification of the significant elements that composed the system – buried pipes, test room and solar chimney. The network considered 11 air nodes for the buried pipes, 4 for the test room and 4 for the solar chimney. While not the most accurate, this type of approach has the advantage of enabling a coupled dynamic simulation for the whole year (Clarke 1997; Hensen, Bartak et al. 2002).The association of the multi-zone model to an airflow network was supported by the "Type 212" component of ESP-r, which is characterized by localized loss coefficients (table 2) and roughness values, taking into consideration the friction resistance of the airflow through the installation (table 3). It was assumed that the vertical air movement between the four layers of the test room is only driven by buoyancy, not being considered any friction resistance. Internal gains were not considered in the simulation model once they did not exist during the test period.

Table 2: Localized loss coefficients of the airflow network (ASHRAE 2005)

Building element	Fitting element	Co (-)
Buried pipes	Entrance	0.50
	Elbow, 90 degrees	0.26
	Discharge	2.00
Solar chimney	Entrance	0.46
	Elbow, 90 degrees	1.27
	Discharge	3.00

Table 3: Roughness of the airflow network elements (Çengel 2003)

Building element	Material	Roughness (mm)
Buried pipes	Concrete	3.00
	PVC	0.03
Solar chimney	Concrete	3.00
	Aluminum	0.03

The monitored data collected included the outdoor climate conditions verified in site during the monitoring procedure. These conditions were used as inputs of the simulation model and allowed the reproduction of the physical conditions at the experimental installation during the monitored time period. The wind and its potential effect were not considered.

INITIAL RESULTS

The experimental installation was object of monitoring during two months. The graphical results here presented – a sample of two days (22nd and 23rd of July) - were taken from the entire collected data to help the result analysis.

Figure 4 presents the measured temperatures in the experimental installation, during the two reference days. The variables have the following meaning:

- T amb, meas: outdoor ambient temperature, measured;
- T indoor, meas: indoor air temperature in the test room, measured;
- T air, in pipe, meas: air temperature measured at 1,5m after the buried pipe entrance, close to the exterior;
- T air, out pipe, meas: air temperature measured at 1 m of the exit of the buried pipe, close to the test room;
- T ground, meas: ground temperature measured in the exterior surface of the buried pipe;
- Solar Radiation, meas; measured horizontal solar radiation.

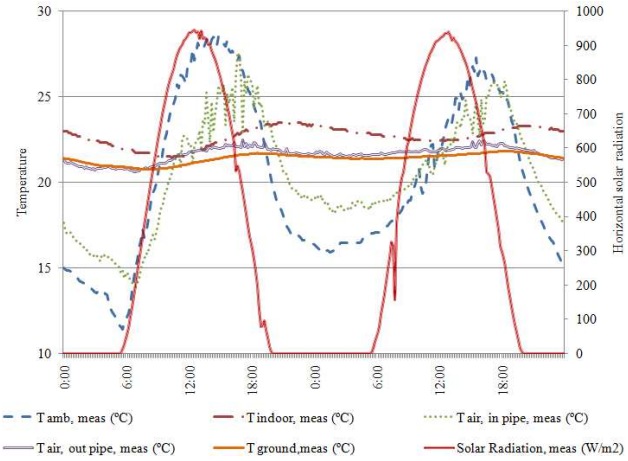

Figure 4: Measured temperatures (22nd and 23rd of July)

The measured indoor temperature into the test room has a very stable behaviour, only presenting some variations between the day and the night periods. As expected the air temperature close to the pipe entrance follows the ambient temperature while the air temperature close to the test room tends to follow the ground temperature. However there are visible

fluctuations and deviations of this temperature during the day, particularly when the ambient temperature is higher.

The simulation model described previously allows the calculation of the indoor temperatures and their comparison with the measured temperatures and also the calculation of the airflow rate circulating in the installation (figure 5). The variables in the graph are:

– T amb, meas: ambient temperature, measured;

– T indoor, meas: indoor air temperature in the test room, measured;

– T indoor, sim: indoor air temperature in the test room, simulated;

– Airflow, sim: induced airflow rate through the solar chimney.

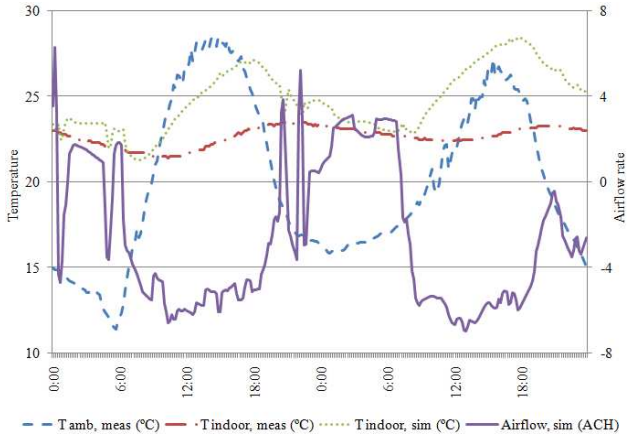

Figure 5: Indoor temperatures and air flow rate through the buried pipes and solar (22nd and 23rd of July)

In figure 5, the airflow that follows the pathway exterior – buried pipes – test room – solar chimney – exterior is considered positive and the airflow that follows the pathway exterior – solar chimney – test room – buried pipes – exterior is considered negative. With this representation it is possible to identify the direction of the airflow rate and its possible interaction with the test room indoor temperature.

The instrumentation existent didn't allow monitoring the airflow rate circulating through the installation. For this reason, there aren't measured values of airflow rate to compare the values of the simulation model with the experimental installation. However, the comparison of the air temperatures in different parts of the buried pipe with the outdoor ambient temperature (T amb) and the ground temperature (T ground) allows the identification of the airflow direction: upwards (pathway exterior – buried pipes – test room – solar chimney – exterior) vs. downwards (pathway exterior – solar chimney – test room – buried pipes – exterior). Therefore, the air temperature (T8) at 4.8m (1/3 of its length) of the pipe entrance was taken and the following criteria were adopted to define the airflow direction during the monitoring period:

→ If $|T_{amb}-T_8| \leq |T_8-T_{ground}|$ is considered upwards airflow;

→ If $|T_{amb}-T_8| > |T_8-T_{ground}|$ is considered downwards airflow.

Following these hypotheses, the graph presented in figure 6 was built, where the value 1 means upwards airflow and the value -1 downwards airflow.

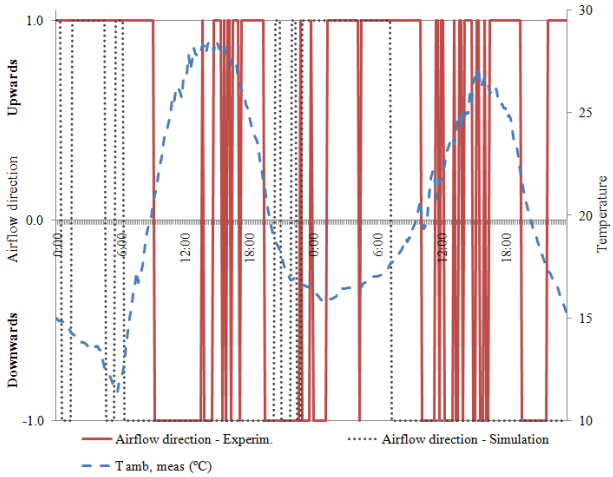

Figure 6: Comparison of the induced airflow direction (22nd and 23rd of July)

This comparison shows that both the measurement and simulation present significant variations in the airflow direction through the day. Its behaviour is mostly upwards during the night period, although frequently and even usually is downwards in the day period when the exterior temperature is higher.

The results' analysis shows that there is no clear accomplishment of the initial purposes for the solar chimney relative to the induction of the airflow rate with upwards direction. It was expected that the solar

chimney induced an upwards airflow rate, at least during the hours with higher solar radiation, what wasn't obtained by the simulation model, neither, in a consistent way, by the experimental installation.

This behaviour can be explained by the lower temperature verified inside the pipes which during the day creates an air density difference contrary to the chimney effect and induces a downwards airflow. The pipes thus create the "inverse chimney effect". The increase of the air temperature in the solar chimney is not high enough for the buoyancy force resulting from the air expansion to oppose the effect referred previously. During the night, the outdoor temperature is much lower than during the day and the indoor temperature of the test room is relatively high when compared with the outdoor temperature. In the buried pipes, the air temperature is decreased, but is not sufficient to oppose the potential force generated in the test room and in the solar chimney. The airflow rate has, therefore, upwards direction.

MODEL CALIBRATION

The experimental results related with the airflow direction in the buried pipes, test room and solar chimney expose the insufficiency of the upwards force induced by the solar chimney and the need of mechanical ventilation to force the upwards airflow.

However, it is recognized that the simulation model is still far from producing accurate results during the day period (figure 6). For that reason an attempt to calibrate the simulation model was performed.

The comparison of both monitored and simulated data provided a base to improve and calibrate the simulation model. A sensitivity study was made, focusing in two fundamental variables of the natural ventilation flows: the localized loss coefficients and the surface convection heat transfer coefficients.

Localized loss coefficients

The localized loss coefficients represent one of the biggest potential for the results deviation. Despite the fact of the localized loss coefficients were the usual for conventional airflow networks (ASHRAE 2005), it is known that there is a significant variability function of the geometric specificities and the flow Reynolds value. Another important argument is that the concept of loss coefficient can vary significantly for very low Reynolds values.

The adopted strategy was to correct the localized loss coefficients indicated by ASHRAE, which were called original localized loss coefficients, using a method proposed by Hooper (Hooper 1981). This method, denominated two-K method, allows the calculation of localized loss coefficients, based on the type of localized loss coefficient and corrected by the airflow velocity. The expression to calculate the loss coefficient function of the airflow velocity is:

$$Co = Co1 / N_{Re} + Co\infty(1 + 1/D) \quad (1)$$

Where Co is the localized loss coefficient, Co_1 and Co_∞ are constants indicated by Hooper, function of the type of localized loss coefficient. N_{Re} is the Reynolds number and D represents the internal diameter of the pipe where the airflow takes place.

Since the Reynolds number are interrelated to the Co, an iterative strategy of two calculation steps was adopted to apply this method, starting with the localized loss coefficient found in the literature (ASHRAE 2005), then applying the two-K method. The results presented in table 4 are relative to the second iteration of the method. The method was applied to the elbow, 90 degree, part of the buried pipes. Based on the calculation of the elbow localized loss coefficient, the resultant correction factor between the original and the new localized loss coefficient was applied to the other localized loss coefficients of the installation. This action is justified by the fact that from the localized loss coefficients of the installation only the elbow, 90 degree, has, from the Two-K method, the necessary constants necessary to the method application. The resulting localized loss coefficients are indicated in the table 5 (row "Corrected Co").

To obtain a clear range of results, more three different global localized loss coefficients variations were also considered (equal to the sum of all localized loss coefficients of the installation), in a logarithmic scale, with values of 20, 200 and 2000. These global values

were split for each localized loss coefficients of the installation, according to the specific weight of each original localized loss coefficient. The value of 2000 was chosen as an extreme value of global loss coefficients, trying to explore the limits of the model reaction to as high as possible range of loss coefficients.

Table 4: Localized loss coefficients – calibration of the air flow network

Co	Buried pipes (-)	Solar chimney (-)	Total (-)
Original Co	2.76	4.73	7.49
Corrected Co	5.95	10.19	16.14
Co 20	7.37	12.63	20
Co 200	73.70	126.30	200
Co 2000	737	1263	2000

The indoor test room temperatures resulting from the application of each localized loss coefficient model into the simulation model are presented in figure 7, for the two July days in analysis.

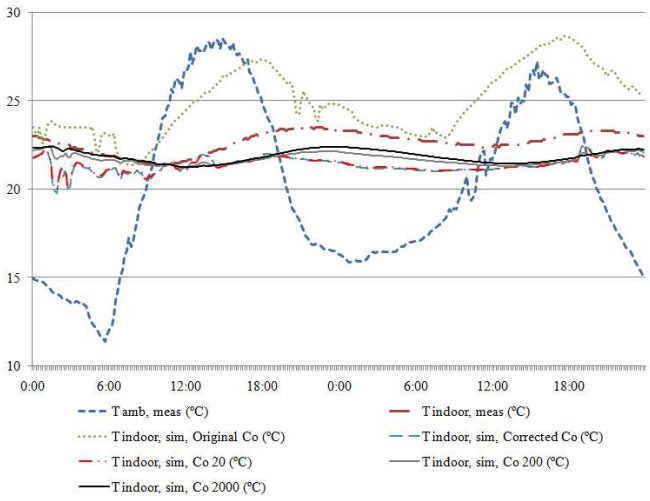

Figure 7: Indoor test room temperatures comparison (22nd and 23rd of July)

The variables in the graph have the following meaning:

- T amb, meas: ambient temperature, measured;
- T indoor, meas: indoor air temperature in the test room, measured;
- T indoor, sim, Original Co: indoor air temperature in the test room with the original localized loss coefficients, simulated;
- T indoor, sim, Corrected Co: indoor air temperature in the test room with the original localized loss coefficients, simulated;
- T indoor, sim, Co 20: indoor air temperature in the test room with the global localized loss coefficients of 20, simulated;
- T indoor, sim, Co 200: indoor air temperature in the test room with the global localized loss coefficients of 200, simulated;
- T indoor, sim, Co 2000: indoor air temperature in the test room with the global localized loss coefficients of 2000, simulated.

To evaluate the differences of the indoor test room temperatures obtained with the monitoring procedure and with the simulation model, the absolute mean deviations were calculated for the entire 2 months in analysis and a results time-step of ten minutes (table 5), computed by:

$$AMD = \frac{\sum_{i=1}^{N} \left| T_{indoor,Measured} - T_{indoor,Simulated} \right|}{N} \quad (2)$$

Table 5: Absolute mean deviation of the indoor temperature (localized loss coefficients)

Co	Localized loss coefficient (-)	AMD July and August(-)
Original Co	7.49	2.51
Corrected Co	16.14	1.76
Co 20	20	1.69
Co 200	200	1.10
Co 2000	2000	1.05

Analyzing the figure 7 and the absolute mean deviation of the indoor test temperature, presented in the table 5, it is possible to identify that the simulated indoor temperature becomes closer to the measured indoor temperature when the localized loss coefficients become higher.

In conclusion, the simulation models which obtain closer experimental installation results are the models that use the localized loss coefficients of Co 200 and Co 2000. Ideally, it should be used localized loss coefficient that could vary, in each time step, function of the Reynolds number. However, limitations of the most part of the building simulation tools don't allow the easy implementation of this parameter modelling the studied natural ventilated system e.g. in ESP-r this requires changing the source code.

Convection heat transfer coefficients

The influence of the convection heat transfer coefficients of the pipes related to the airflow velocity was also considered. The heat transfer into the buried pipes is dominated by the convection process between the pipes walls and the airflow circulating through the pipes. Therefore, the calculation of the convection coefficients is critical for accuracy results.

The modelling of the buried pipes shape was simplified, using a square shape instead of a circular original (experimental installation) shape. The first approach of the simulation model modelling was done using the Alamdari and Hammond method, presented by Beausoleil-Morrison, (Beausoleil-Morrison 2000), expressions 3 and 4. This correlation was considered because it is the correlation used by ESP-r by default (and many modelers don't even change from the default option), so it somehow constitutes a base-case for comparison.

Vertical surfaces of the pipe:

$$h_c = \left\{ 1.5 \left[\left(\frac{\Delta T}{H} \right)^{1.4} \right]^6 + \left[1.23 \Delta T^{1/3} \right]^6 \right\}^{1/6} \quad \left(W / m^2 K \right) \quad (3)$$

Horizontal surfaces of the pipe:

$$h_c = \left\{ 1.4 \left[\left(\frac{\Delta T}{D_h} \right)^{1.4} \right]^6 + \left[1.63 \Delta T^{1/3} \right]^6 \right\}^{1/6} \quad \left(W / m^2 K \right) \quad (4)$$

These correlations express the convection coefficient (hc) as function of the surface´s characteristic dimension (H (m) – height of the surface (m) and Dh (m) – hydraulic diameter of the pipe) and the surface-air temperature difference (ΔT (ºC)). The correlations here presented represent heat exchange between a generic room air and the solid surfaces of that room, for buoyancy-driven flows.

Alternative correlations more appropriate to the phenomena of fluid flows in pipes were found in the literature The expressions 5 and 6 are proposed by Çengel (Çengel 2003) for laminar and turbulent flows in pipes, fully developed, and with constant surface temperatures.

Vertical and horizontal surfaces of the pipe:

$$h_c = \frac{3.66 \times k}{D_h}, \text{ if Re } < 10\,000 \text{ "Re"} \quad \left(W / m^2 K \right) \quad (5)$$

- Reynolds number, "k" -conductivity of the pipe wall, "Nu" - Nussel number.

$$h_c = \frac{0.023 \times \mathrm{Re}^{0.8} \times \mathrm{Pr}^n \times k}{D_h},$$

if Re > 10 000 and 0,7 ≤ Pr ≤ 160, with n=0.4 for heating and 0.3 for cooling of the fluid flowing through the pipe. "Pr" - Prandtl number $\left(W / m^2 K \right)$ (6)

The main difference between both correlations is the consideration of the air velocity in the convection coefficient by the method proposed by Çengel, while the Alamdari and Hammond method is applicable, as referred by Beausoleil-Morrison, where buoyancy is caused only by a temperature difference between a surface and the surrounding room air. In the studied system, buried pipes associated with a solar chimney, a considerable amount of airflow can be induced by the natural ventilation system, with significant air velocity inside the buried pipes (up to 0.7m/s).

To study the sensitivity of both methods the airflow velocity inside the buried pipes was observed through the two months and the convection heat transfer coefficients were computed, using both Alamdari and Hammond and Çengel methods (figure 8).

There are significant differences between the convection coefficients obtained from the two methods: the Çengel method finds convection heat transfer coefficients that are about four (laminar airflow) to eighty times (turbulent airflow) bigger than the coefficients found by the Alamdari and Hammond method. In practice the results showed that both situations of laminar and of turbulent flow can occur.

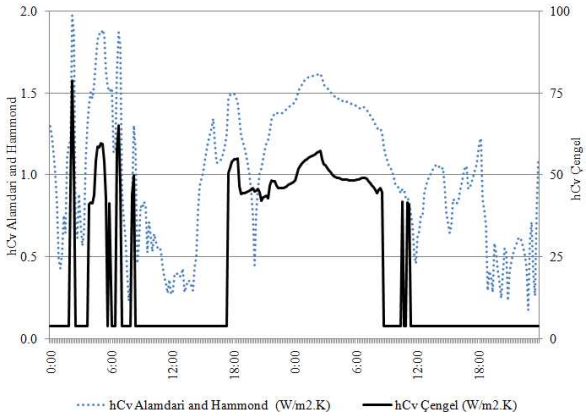

Figure 8: Convection heat transfer coefficients

To assess the impact of these coefficients in the system performance – indoor temperatures – it was applied the mean value of the convection heat transfer coefficients, calculated by the Çengel method for the reference installation, 13W/m^2.K, in the modelled buried pipes system (figure 9) and performed with the option "Original Co" of table 5.

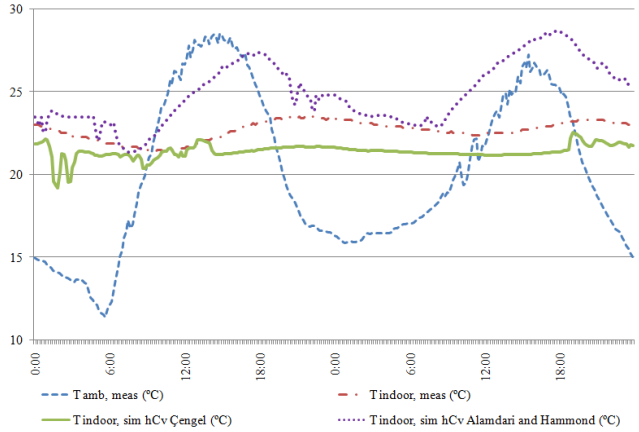

Figure 9: Indoor temperatures comparison, using both coefficient calculation methods (22nd and 23rd of July)

The simulated temperatures obtained through the Çengel method are much closer of the measured indoor temperatures than the obtained through the Alamdari and Hammond method. In the table 6 are presented the absolute mean deviation of the indoor temperature for both studied months and both calculation methods.

Table 6: Absolute mean deviation of the indoor temperature (convection heat transfer coefficients)

Convection coefficients method	**AMD July and August(-)**
Alamdari and Hammond (expressions 3 and 4)	2.51
Çengel (expressions 5 and 6)	1.71

The Çengel method and the consideration of the airflow velocity instead the Alamdari and Hammond method permit obtaining indoor temperatures that are much closer than the experimental installation. However, the Çengel method wasn't applied dynamically in the simulation model for software limitations (it would imply changes to the source code).

CONCLUSIONS

The system composed by buried pipes and solar chimney has demonstrated, for the Portuguese climate, clear difficulties to promote a natural airflow in the hours with higher ambient temperatures.

In terms of modelling, it was found that the airflow velocity in the buried pipes and the system performance are strongly connected with the localized loss coefficients and the heat convection coefficients associated with the airflow network.

It was possible to achieve a model that reproduces reasonably the system behaviour. Nevertheless, it would be desirable to introduce more dynamic options in the whole-building simulations software, especially the options related to convective heat transfer processes and localized loss coefficients, which are important to modelling uncommon or innovative building elements.

REFERENCES

ASHRAE (2005). ASHRAE Handbook - Fundamentals, American Society of Heating, Refrigerating and Air-Conditioning Engineers, Inc.

Beausoleil-Morrison (2000). The Adaptive Coupling of Heat and Air Flow Modelling Within Dynamic Whole-Building Simulation. Energy Systems Research Unit. Glasgow UK, University of Strathclyde. **Doctoral Dissertation**.

Çengel, Y. A. (2003). Heat Transfer: A Practical Approach, McGraw Hill.

Clarke, J. A. (1997). The simulation of photovoltaic-integrated building façades. Fifth International IBPSA Conference. Prague, Czech Republic.

Clarke, J. A. (2001). Energy simulation in building design. Bristol, Butterworth-Heinemann.

Hensen, J., M. Bartak, et al. (2002). Modeling and simulation of a double-skin façade system. ASHRAE Transactions 2002. Honolulu, HI, United States, American Soc. Heat. Ref. Air-Conditioning Eng. Inc.**:** 22-26.

Hooper, W. B. (1981). "The Two-K Method." Chemical Engineering **88**.